Volume 59
Number 71
14 September 2023
Pages 10563–10678

ChemComm

Chemical Communications

rsc.li/chemcomm

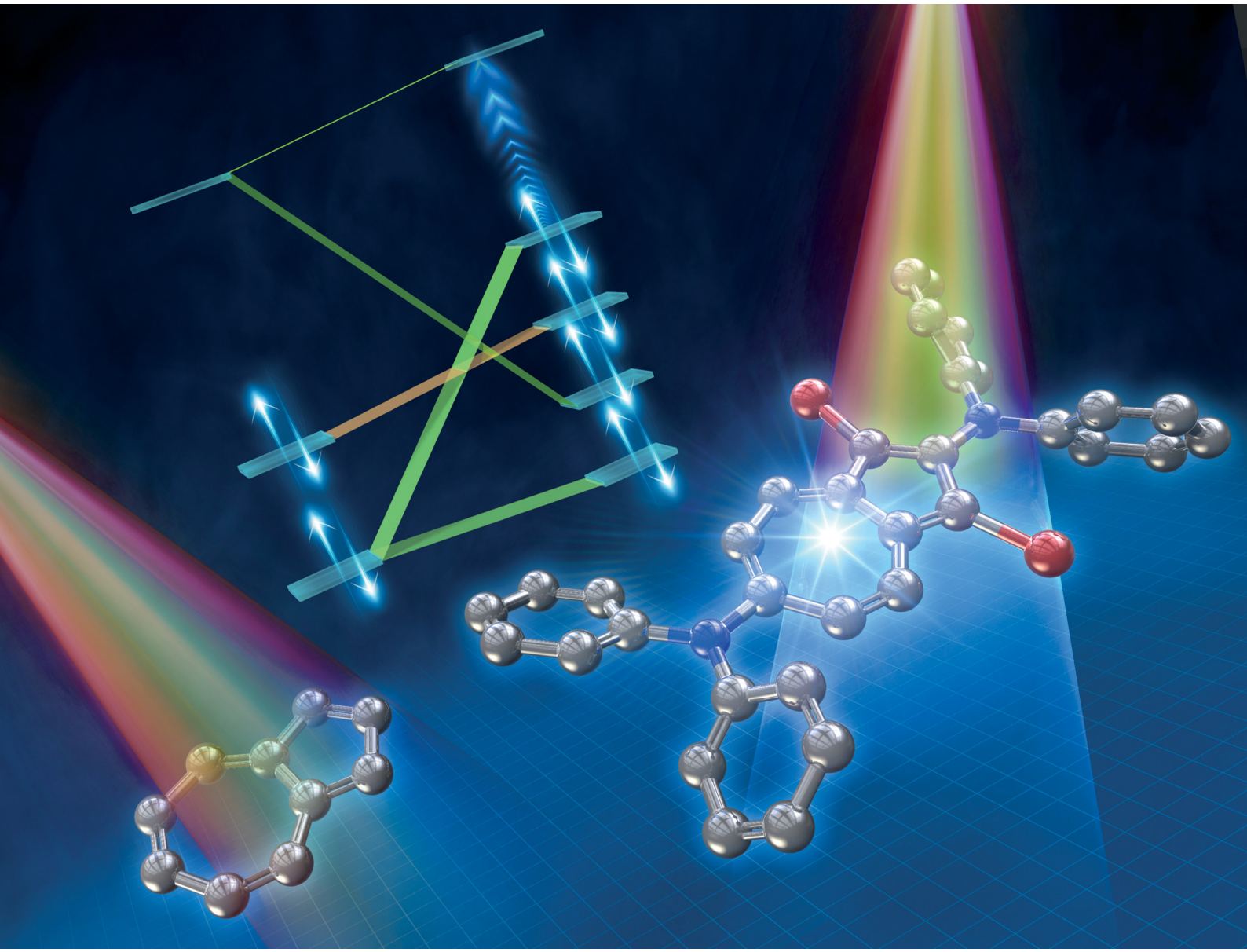

ISSN 1359-7345

ROYAL SOCIETY OF CHEMISTRY

COMMUNICATION

Takahiro Tsuchiya, Yasuhiro Mazaki *et al.*

Intense absorption of azulene realized by molecular orbital inversion

ChemComm

COMMUNICATION

View Article Online
View Journal | View Issue

Cite this: *Chem. Commun.*, 2023, **59**, 10604

Received 12th May 2023,
Accepted 25th July 2023

DOI: 10.1039/d3cc02311g

rsc.li/chemcomm

Intense absorption of azulene realized by molecular orbital inversion†

Takahiro Tsuchiya,*[a] Tomohiro Hamano,[a] Masahiro Inoue,[a] Tomoya Nakamura,[b] Atsushi Wakamiya[b] and Yasuhiro Mazaki*[a]

The introduction of diarylamino groups at the 2- and 6-positions of azulene was found to invert the order of the orbital energy levels and allowed the HOMO–LUMO transition, resulting in a substantial increase in absorbance in the visible region. In addition, the stability of their one-electron oxidised species was improved by introducing bromine or methoxy groups at the 1- and 3-positions.

Benzene and acenes, such as naphthalene and anthracene, display excellent electron-donating properties when they contain substituted bis(diarylamino) groups[1–10] and have garnered interest due to their potential applications such as organic semiconductors,[1] multi-electron redox materials[2–4] for rechargeable batteries,[5,6] chromophore linkers for nonlinear optically active metal–organic framework (MOF) materials,[7] and dopants in the emitting layers for organic light-emitting devices (OLEDs).[8] These substituted acenes are also attracting attention because of their ability to absorb visible light, which enables them to be used as photoreduction catalysts.[9,10] Furthermore, azulene[11–20] is a structural isomer of naphthalene, with relatively high HOMO and low LUMO energy levels due to its unique polarisation structure (Fig. 1a), and it is also known as a redox-active molecule compared to naphthalene, anthracene, pyrene and so on.[11–15] In this context, hole-transporting materials with a two-dimensionally expanded π-system around the azulene core for efficient perovskite solar cells have also recently attracted interest.[21,22] In addition, 1,3-bis(diarylamino)azulene **1** (Scheme 1a) is reported to exhibit high electron-donating properties.[23] However, we are not aware of a system in which diarylamino groups have been introduced at the 2- and 6-positions of azulene. The 1- and 3-positions of azulene have large HOMO coefficients, while the 2- and 6-positions have large HOMO−1 and LUMO coefficients (Fig. 1b).[11–15] Hence, it is conceivable that the electronic structure of azulene changes significantly depending on the positions where the diarylamino groups are introduced.

Azulene exhibits a bright-blue colour and shows absorption derived from the S_0–S_1 transition at approximately 580 nm.[24] However, its molar-absorption coefficient is approximately 350 M^{-1} cm^{-1}, which is very weak for π–π* transition absorption (Fig. 1c, left).[24] This is due to the forbidden HOMO–LUMO transition; the HOMO of azulene is distributed across its odd-positioned carbon atoms, while the coefficients of the LUMO and HOMO−1 are greater in its even-positioned carbon atoms. Therefore, the ability to control the molecular-orbital (MO) energy levels of azulene will lead to the creation of a material having new optical and electronic characteristics (Fig. 1c, right).

In this study, we introduced diarylamino groups at the azulene 2- and 6-positions of compound **2**, and then investigated its optical properties and redox behaviour. Moreover, we evaluated the stabilisation of the one-electron oxidised species of **3**, in which methoxy groups were introduced at the 1- and 3-positions of azulene.

The synthesis of **1** through the reaction between 1,3-dibromoazulene[25] and diarylamine has previously been

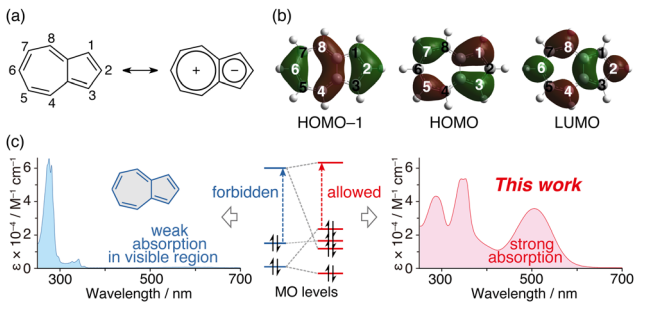

Fig. 1 (a) Numbering of atoms in azulene and its polarized resonance structure. (b) HOMO−1, HOMO and LUMO of azulene. (c) Concept for molecular-orbital inverted azulene possessing strong absorption of visible light.

[a] *Department of Chemistry, Kitasato University Kitasato 1-15-1, Sagamihara, Kanagawa 252-0373, Japan. E-mail: ttsuchi@kitasato-u.ac.jp*
[b] *Institute for Chemical Research, Kyoto University Uji, Kyoto 611-0011, Japan*

† Electronic supplementary information (ESI) available. CCDC 2254119, 2254124, 2254133, and 2254134. For ESI and crystallographic data in CIF or other electronic format see DOI: https://doi.org/10.1039/d3cc02311g

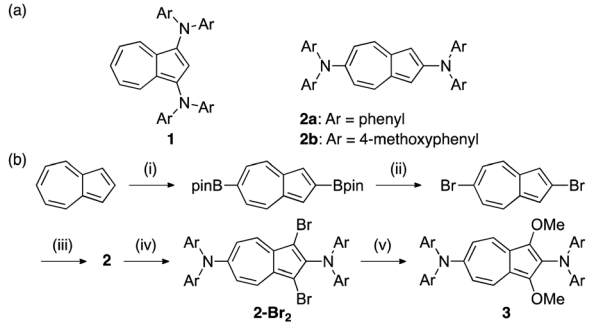

Scheme 1 (a) Structural formulae of **1** and **2**. (b) Synthesis of **2**, **2-Br$_2$** and **3**. *Reagents and conditions*: (i) pin_2B_2, $[IrCl(cod)]_2$, bpy, cyclohexane, reflux, 48 h, 45%; (ii) CuBr, DMF, 80 °C, 2 h, 88%; (iii) Ar_2NH, $Pd(OAc)_2$, ^tBuOK, $^tBu_3PHBF_4$, toluene, reflux, 2 h, **2a**: 80%, **2b**: 82%; (iv) NBS, $CHCl_3$, −78 °C, 2 h, **2a-Br$_2$** : 82%, **2b-Br$_2$** : 84%; (v) MeONa, CuBr, MeOH, DMF, 100 °C, 5 d, **3a**: 74%, **3b**: 58%.

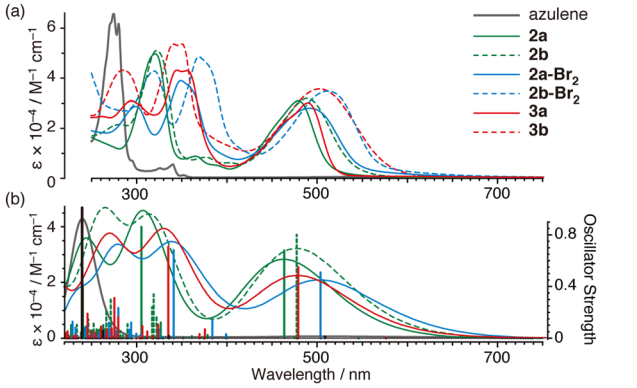

Fig. 2 (a) UV-Vis absorption spectra of azulene (black line), **2** (green line), **2-Br$_2$** (blue line) and **3** (red line) in THF. (b) Simulated absorption spectra at the TD-B3LYP/6-31G(d)//B3LYP/6-31G(d) level.

reported.[23] Although 1,3-dibromoazulene can be obtained by the reaction of azulene with *N*-bromosuccinimide (NBS),[25] a precursor of **2**, 2,6-dibromoazulene, has been conventionally synthesised from α-tropolone in five steps (14% overall yield).[26,27] One of the factors that made the synthesis of **2** difficult is the complicated route of raw material synthesis. However, recent reports have shown the successful borylation of the 2- and 6-positions of azulene through its iridium-catalysed reaction with bis(pinacolato)diboron (B_2pin_2).[28] Hence, in the present study, we synthesised 2,6-dibromoazulene through bromination of 2,6-diborylazulene (Scheme 1b).

The reaction of the obtained diborylazulene with copper bromide gave dibromoazulene with a yield of 92%. Subsequently, **2** was formed by a coupling reaction between dibromoazulene and diarylamine in toluene, in the presence of a Pd-catalyst. Bromination with NBS was used to introduce substituents at positions 1 and 3 for compound **2**. Subsequently, 1,3-dimethoxy compound **3** was obtained by reacting the dibromide compound with sodium methoxide in methanol in the presence of copper bromide.

Compounds **2**, **2-Br$_2$**, and **3** were characterized by NMR measurements (Fig. S1–S9, ESI†). Interestingly, in the ^{1}H NMR spectrum of **2a** in $CDCl_3$, the *ortho*- and *meta*-position phenyl signals of the diphenylamino group at the 2-position of azulene were observed to be equivalent (Fig. S2a, S3, and S4, ESI†). This is a peculiar phenomenon in $CDCl_3$, and when the solvent was changed to acetone-d_6, the signals did not appear to be equivalent (Fig. S2b–S2e, ESI†). It is possible that the signals overlapped to produce something that resembles this multiplet in $CDCl_3$.

Single crystal X-ray structure analysis was conducted on compounds **2a**, **2a-Br$_2$**, **2b**, and **2b-Br$_2$** (Fig. S10–S13, ESI†). The asymmetric unit of **2-Br$_2$** was one molecule, whereas for **2** there was disorder, where the five-membered and seven-membered rings of azulene were inverted, and the asymmetric unit contained half a molecule. Each amino group nitrogen of **2** and **2-Br$_2$** had an almost planar structure, and the dihedral angle between the azulene and amino-group planes was 24° in **2a** and 28° in **2b**, while in **2-Br$_2$**, the dihedral angles were significantly different between the 5-membered- and 7-membered-ring sides, 65° and 13° in **2a-Br$_2$** and 67° and 13° in **2b-Br$_2$**, respectively. It was concluded that the dihedral angle on the 2-position side was large because of the steric repulsion between the bromines at the 1- and 3-positions and the phenyl groups. The carbon–carbon bonds of the azulene skeleton tended to elongate slightly around the introduction position of the diarylamino group and bromine.

Compounds **2**, **2-Br$_2$**, and **3** exhibit brown or reddish-orange colours, which are significantly different from that of the raw material azulene (blue colour). All ultraviolet-visible (UV-Vis) absorption spectra showed absorption bands near 400 to 700 nm (**2a:** λ_{max} 480 nm, ε 31 500 M^{-1} cm^{-1}; **2b:** λ_{max} 490 nm, ε 31 700; **2a-Br$_2$:** λ_{max} 492 nm, ε 28 300, **2b-Br$_2$:** λ_{max} 516 nm, ε 34 600; **3a:** λ_{max} 494 nm, ε 31 000; and **3b:** λ_{max} 506 nm, ε 37 300) in tetrahydrofuran (THF) as shown in Fig. 2a. Absorption in these visible light regions (ε 28 300–37 300 M^{-1} cm^{-1}) is much stronger than by azulene (S_0–S_2, λ_{max} 340 nm, ε 4000 M^{-1} cm^{-1}; S_0–S_1, λ_{max} 580 nm, ε 350)[24] and also the previously reported 1,3-bis(diphenylamino)azulene (**1**) (λ_{max} 420 nm, ε 10 000 M^{-1} cm^{-1}; λ_{max} 667 nm, ε 300).[23] These absorption bands of **2**, **2-Br$_2$**, and **3** are distributed at similar or longer wavelengths than those of oligothiophenes (P3HT: 455 nm;[29] MK-2: λ_{max} 480 nm, ε 38 400 M^{-1} cm^{-1};[30] MK-3: λ_{max} 485 nm, ε 40 100;[30] and MK-4: λ_{max} 474 nm, ε 33 100[30]), which are commercially available as organic dyes for dye-sensitised solar cells, and 1,4-bis(diphenylamino)naphthalene (λ_{max} 375 nm, ε 9200 M^{-1} cm^{-1}),[10] which has been used as a photoreduction catalyst under visible light. The absorption spectra of **2**, **2-Br$_2$**, and **3** showed relatively good agreement with the results of calculations thus using time-dependent density-functional theory (TDDFT) (Fig. 2b), indicating that the strong absorption in the visible light region is derived from the allowed HOMO–LUMO transition (Fig. 3).

Fig. 3 shows the MO diagram of azulene, diphenylamine, **1**, and **2a**. Since the 2- and 6-positions of azulene are located in the HOMO node, the introduction of diphenylamino groups at the 2- and 6-positions does not affect the HOMO; however, it is

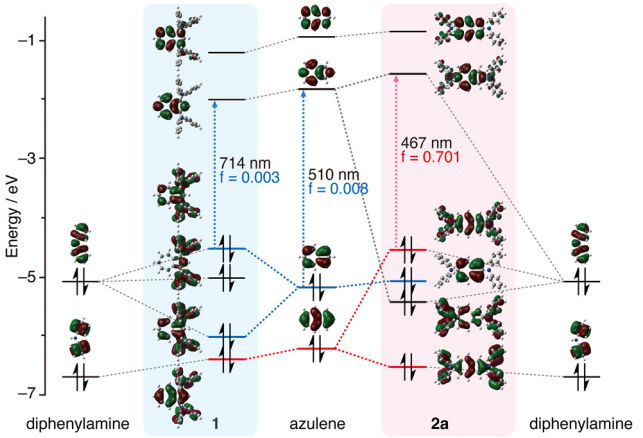

Fig. 3 MO diagrams of azulene, diphenylamine, **1** and **2a** calculated at the B3LYP/6-31(d) level.

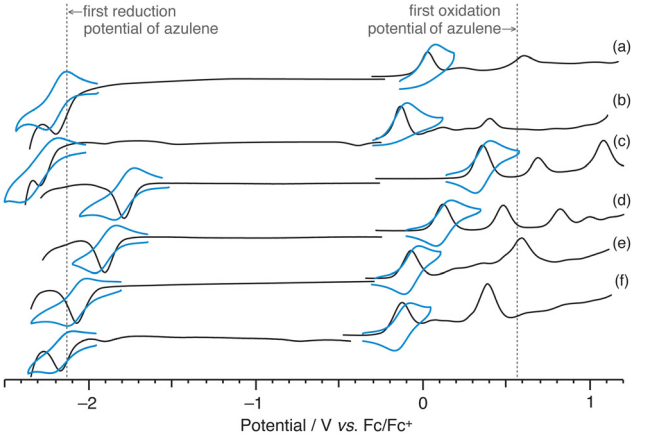

Fig. 4 Square-wave voltammogram (SWV, black line) and cyclic voltammogram (CV, blue line) of (a) **2a**, (b) **2b**, (c) **2a-Br$_2$**, (d) **2b-Br$_2$**, (e) **3a** and (f) **3b**.

shown that the HOMO−1 and LUMO of azulene strongly form a linear combination with the HOMO of diphenylamine. Consequently, the HOMO of **2a** is distributed in both the azulene skeleton and the diphenylamino group, and is formed by the antibonding interaction between the HOMO−1 of azulene and the HOMO of diphenylamine. And the HOMO of **2a** is located at a higher level (destabilised) than that of the original azulene. This means that the order of the MO energy levels is inverted between azulene and **2a**. As a result, it is conceivable that the HOMO–LUMO transition of **2a** is allowed because it is a transition between orbitals with a large coefficient on even-numbered carbons, resulting in stronger absorption in the long-wavelength region. Introduction of one diphenylamino group at the 2- or 6-position of azulene also forms a linear combination of the HOMO−1 of azulene with the HOMO of diphenylamine (Fig. S14, ESI†). However, the interactions are weaker than when doubly substituted, and the LUMO of azulene does not form a linear combination with the HOMO of diphenylamine unlike **2**. As a result, the HOMO energy levels of 2- and 6-(diphenylamino)azulene are lower than that of **2**.

In **1**, the HOMO of the azulene forms a linear combination with the HOMO of diphenylamine (Fig. 3). The HOMO of **1** is also higher in energy than that of the original azulene, thus reducing the HOMO–LUMO gap. Despite this, the HOMO–LUMO transition of **1** remains forbidden. On the other hand, the order of the MO energy levels is consistent among **2**, **2-Br$_2$** and **3**, and the HOMO–LUMO transitions of the compounds are all allowed (Fig. S15, ESI†). Introduction of methoxy groups at the *para*-positions of the diphenylamino groups leads to an overall energy increase in the MO levels except for HOMO−1 (Fig. S16, ESI†).

Redox potential measurements were taken to examine the electronic properties in detail (Fig. 4 and Table S8, ESI†). The first *reduction* potential of **2a** ($^{red}E_1$: −2.16 V *vs.* Fc/Fc$^+$) showed a value similar to that of azulene ($^{red}E_1$: −2.13 V), whereas the first *oxidation* potential of **2a** ($^{ox}E_1$: 0.03 V) had a cathodic shift of about 500 mV *vs.* Fc/Fc$^+$ relative to that of azulene ($^{ox}E_1$: 0.56 V). The oxidation potential of 2,6-bis(diphenylamino)naphthalene is reportedly 0.24 V,[8] indicating that **2a** has a higher electron donating capacity. Moreover, compared with **2a**, **2b** ($^{ox}E_1$: −0.12 V, $^{red}E_1$: −2.28 V) had a cathodic shift of about 100 mV for both oxidation and reduction potentials, and the electron donating ability was further improved. These results are consistent with the results of DFT calculations.

Although the first *reduction* waves of **2** showed reversible behaviour in cyclic voltammetry (CV) (Fig. 4a and b, blue lines), the reversibility of the first *oxidation* processes was not observed. In contrast, it was found that the first oxidation processes of **2-Br$_2$** (**2a-Br$_2$**: 0.36 V, **2b-Br$_2$**: 0.10 V) and **3** (**3a**: −0.07 V, **3b**: −0.14 V), which possess the functional groups at 1,3-positions, were reversible, and the electron donating ability of **3** was more significant than that of **2**. It is known that the irreversible behaviour of the first oxidation process is characteristic of azulene, and that the radical cations of azulene polymerise at the 1,3-positions where the HOMO coefficient is large.[31] Although the spin density of the radical cation of **2** is spread throughout the molecule (Fig. S17, ESI†), it is shown that the spin density at the 1,3-positions is still relatively high. We believe that by introducing substituents at the 1,3-positions like **2-Br$_2$** and **3**, the polymerisation at these positions was suppressed and reversibility appeared.

The morphology and electronic characteristics of the azulene derivatives in the thin film were also investigated. Atomic force microscopy (AFM) measurements for the spin-coated samples showed a relatively uniform and flat surface (Fig. S18, ESI†). The UV-Vis absorption spectra of **2** and **2a-Br$_2$** in the spin-coated films exhibited a shape similar to those in solution (Fig. 5a), but the absorption in the visible region was shifted by about 13 to 24 nm to longer wavelengths than those in solution. Since the mixed film with poly(methyl methacrylate) (PMMA) showed absorption at almost the same position as that in the solution, it was concluded that the long wavelength shift was caused by intermolecular interactions between the azulene derivatives in the solid state.

The ionic potentials of **2** in the spin-coated thin-film state were determined by photoelectron yield spectroscopy (PYS)

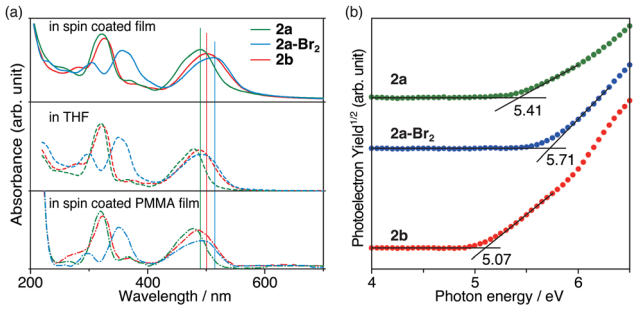

Fig. 5 (a) UV-Vis absorption spectra in spin coated film, THF, and spin coated PMMA film and (b) PYS spectra of **2a** (green), **2a-Br$_2$** (blue), and **2b** (red).

measurements under vacuum (Fig. 5b). The HOMO energies of the thin films of **2a**, **2a-Br$_2$** and **2b** were found to be −5.41, −5.71 and −5.07 eV, respectively. These values are comparable to those of prevalently used hole transporting materials [2,2′,7,7′-tetrakis(*N*,*N*-di-*p*-methoxyphenylamine)-9,9′-spirobifluorene (spiro-OMeTAD): −5.05 eV;[32] poly[bis(4-phenyl)(2,4,6-trimethylphenyl) amine] (PTAA): −5.1 eV;[33] poly(3,4-ethylenedioxythiophene)polystyrene sulfonate (PEDOT:PSS): −5.1 eV;[34] and azulene-core-based two-dimensionally expanded π-systems: −4.96 to −5.00 eV[21]] for solid-state dye-sensitized solar cells (ssDSSCs) and perovskite solar cells (PSCs).

In conclusion, we successfully synthesised azulene-based organic electron donors that strongly absorb visible light. This was achieved by introducing electron-donating substituents at the 2- and 6-positions of azulene, resulting in an inversion of the orbital energy level order of original azulene and permitting its previously forbidden HOMO–LUMO transition. Furthermore, it was confirmed that their one-electron oxidised species could be stabilised by introducing a substituent at the 1- and 3-positions. Compounds **2** and **3** have higher HOMOs than metal porphyrins and thiophene trimers and tetramers and exhibit strong absorption properties over a wide range of wavelengths. Therefore, we believe that these findings provide a rational approach to constructing a wide variety of azulene-based π-conjugated molecules for photonic, optoelectronic, and photocatalytic applications.

This work was supported by the International Collaborative Research Program of Institute for Chemical Research, Kyoto University (grant # 2022-22).

Conflicts of interest

There are no conflicts to declare.

Notes and references

1 J. Freudenberg, D. Jansch, F. Hinkel and U. H. F. Bunz, *Chem. Rev.*, 2018, **118**, 5598.
2 M. Roy, J. H. Walton, J. C. Fettinger and A. L. Balch, *Chem. – Eur. J.*, 2022, **28**, e202104631.
3 J. Zhang, Z. Chen, L. Yang, F.-F. Pan, G.-A. Yu, J. Yin and S. H. Liu, *Sci. Rep.*, 2016, **6**, 1.
4 X. Wang, Z. Zhang, Y. Song, Y. Su and X. Wang, *Chem. Commun.*, 2015, **51**, 11822.
5 G. Wang, E. Dmitrieva, B. Kohn, U. Scheler, Y. Liu, V. Tkachova, L. Yang, Y. Fu, J. Ma and P. Zhang, *Angew. Chem., Int. Ed.*, 2022, **61**, e202116194.
6 Y. Chen, X. Gao, L. R. Johnson and P. G. Bruce, *Nat. Commun.*, 2018, **9**, 1.
7 D. C. Mayer, A. Manzi, R. Medishetty, B. Winkler, C. Schneider, G. Kieslich, A. Pöthig, J. Feldmann and R. A. Fischer, *J. Am. Chem. Soc.*, 2019, **141**, 11594.
8 C. Wu, P. I. Djurovich and M. E. Thompson, *Adv. Funct. Mater.*, 2009, **19**, 3157.
9 R. Taniguchi, N. Noto, S. Tanaka, K. Takahashi, S. K. Sarkar, R. Oyama, M. Abe, T. Koike and M. Akita, *Chem. Commun.*, 2021, **57**, 2609.
10 N. Noto, T. Koike and M. Akita, *ACS Catal.*, 2019, **9**, 4382.
11 T. Tsuchiya, M. Higashibeppu and Y. Mazaki, *ChemistryOpen*, 2023, **12**, e202100298, DOI: 10.1002/open.202100298.
12 T. Tsuchiya, Y. Katsuoka, K. Yoza, H. Sato and Y. Mazaki, *ChemPlusChem*, 2019, **84**, 1659.
13 T. Tsuchiya, R. Umemura, M. Kaminaga, S. Kushida, K. Ohkubo, S. I. Noro and Y. Mazaki, *ChemPlusChem*, 2019, **84**, 655.
14 A. Konishi and M. Yasuda, *Chem. Lett.*, 2021, **50**, 195.
15 H. Xin, B. Hou and X. Gao, *Acc. Chem. Res.*, 2021, **54**, 1737.
16 A. H. Elwahy and K. Hafner, *Asian J. Org. Chem.*, 2021, **10**, 2010.
17 P. Bakun, B. Czarczynska-Goslinska, T. Goslinski and S. Lijewski, *Med. Chem. Res.*, 2021, **30**, 834.
18 A. G. Lvov and A. Bredihhin, *Org. Biomol. Chem.*, 2021, **19**, 4460.
19 L. C. Murfin and S. E. Lewis, *Molecules*, 2021, **26**, 353.
20 T. Shoji, S. Ito and M. Yasunami, *Int. J. Mol. Sci.*, 2021, **22**, 10686.
21 M. A. Truong, J. Lee, T. Nakamura, J. Y. Seo, M. Jung, M. Ozaki, A. Shimazaki, N. Shioya, T. Hasegawa, Y. Murata, S. M. Zakeeruddin, M. Grätzel, R. Murdey and A. Wakamiya, *Chem. – Eur. J.*, 2019, **25**, 6741.
22 H. Nishimura, N. Ishida, A. Shimazaki, A. Wakamiya, A. Saeki, L. T. Scott and Y. Murata, *J. Am. Chem. Soc.*, 2015, **137**, 15656.
23 G. Nöll, S. Amthor, M. Avola, C. Lambert and J. Daub, *J. Phys. Chem. C*, 2007, **111**, 3512.
24 S. V. Shevyakov, H. Li, R. Muthyala, A. E. Asato, J. C. Croney, D. M. Jameson and R. S. Liu, *J. Phys. Chem. A*, 2003, **107**, 3295.
25 A. Ito, M. Watanabe, A. Ishii, R. Yamasaki and I. Okamoto, *Tetrahedron Lett.*, 2021, **86**, 153523.
26 Q. Fan, D. Martin-Jimenez, D. Ebeling, C. K. Krug, L. Brechmann, C. Kohlmeyer, G. Hilt, W. Hieringer, A. Schirmeisen and J. M. Gottfried, *J. Am. Chem. Soc.*, 2019, **141**, 17713.
27 F. Schwarz, M. Koch, G. Kastlunger, H. Berke, R. Stadler, K. Venkatesan and E. Lörtscher, *Angew. Chem., Int. Ed.*, 2016, **55**, 11781.
28 M. Narita, T. Murafuji, S. Yamashita, M. Fujinaga, K. Hiyama, Y. Oka, F. Tani, S. Kamijo and K. Ishiguro, *J. Org. Chem.*, 2018, **83**, 1298.
29 K. Rahimi, I. Botiz, J. O. Agumba, S. Motamen, N. Stingelin and G. Reiter, *RSC Adv.*, 2014, **4**, 11121.
30 Z.-S. Wang, N. Koumura, Y. Cui, M. Takahashi, H. Sekiguchi, A. Mori, T. Kubo, A. Furube and K. Hara, *Chem. Mater.*, 2008, **20**, 3993.
31 M. Saitoh, J. Yano, T. Nakazawa, Y. Sugihara and K. Hashimoto, *J. Electroanal. Chem.*, 1996, **418**, 139.
32 W. H. Nguyen, C. D. Bailie, E. L. Unger and M. D. McGehee, *J. Am. Chem. Soc.*, 2014, **136**, 10996.
33 S. Zhang, M. Stolterfoht, A. Armin, Q. Lin, F. Zu, J. Sobus, H. Jin, N. Koch, P. Meredith and P. L. Burn, *ACS Appl. Mater. Interfaces*, 2018, **10**, 21681.
34 F. Hermerschmidt, F. Mathies, V. R. Schröder, C. Rehermann, N. Z. Morales, E. L. Unger and E. J. List-Kratochvil, *Mater. Horiz.*, 2020, **7**, 1773.